Supporting Information

Mechanical stability of flexible graphene-based displays

*George Anagnostopoulos[1], Panagiotis-Nektarios Pappas[1], Zheling Li[2], Ian A. Kinloch[2], Robert J. Young[2], Kostya S. Novoselov[3], Ching Yu Lu[4], Nicola Pugno[5], John Parthenios[1], Costas Galiotis[1,6,]*and Konstantinos Papagelis[1,7,]**

[1]Institute of Chemical Engineering Sciences, Foundation for Research and Technology – Hellas (FORTH/ ICE-HT), Patras 265 04, Greece

[2]School of Materials, University of Manchester, Oxford Road, Manchester, M13 9PL, UK

[3]School of Physics and Astronomy, University of Manchester, Oxford Road, Manchester, M13 9PL, UK

[4]BGT Materials Limited, 2.312 Photon Science Institute, University of Manchester, Oxford Road, Manchester, M13 9PL, UK

[5]Laboratory of Bio-Inspired and Graphene Nanomechanics, Department of Civil, Environmental and Mechanical Engineering, University of Trento, Via Mesiano 77, I-38123 Trento, Italy

Center for Materials and Microsystems, Fondazione Bruno Kessler - I-38123 Trento, Italy

School of Engineering and Materials Science, Queen Mary University of London – Mile End Road, London, E1 4NS, UK

[6]Department of Chemical Engineering, University of Patras, Patras 26504, Greece

[7]Department of Materials Science, University of Patras, Patras 26504, Greece

Corresponding Author

*Whom all correspondence should be sent to: c.galiotis@iceht.forth.gr, kpapag@upatras.gr

Table of Contents

1. Depth profile mapping

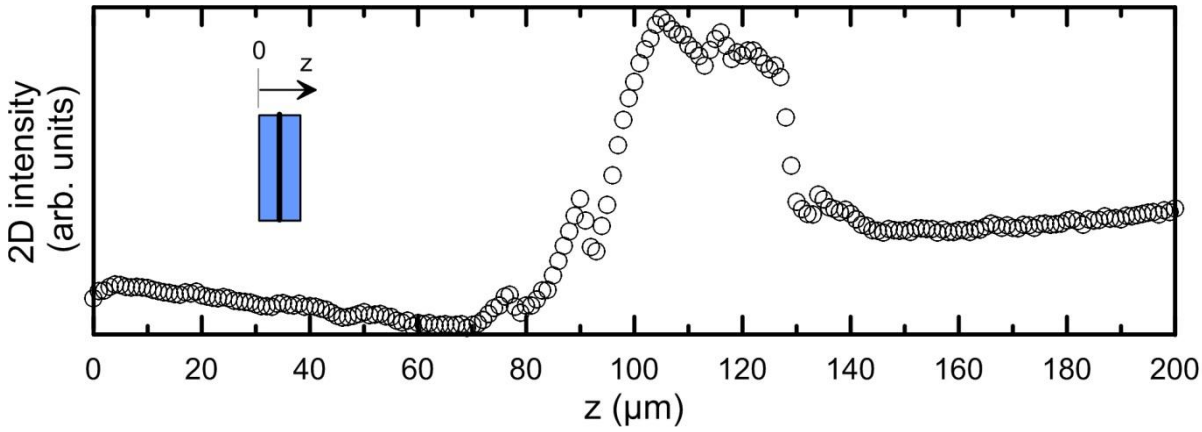

Figure S1: 2D Raman depth profile mapping to identify the exact position of the embedded graphene layers.

2. Spectra evolution of 2D band for various types of loading

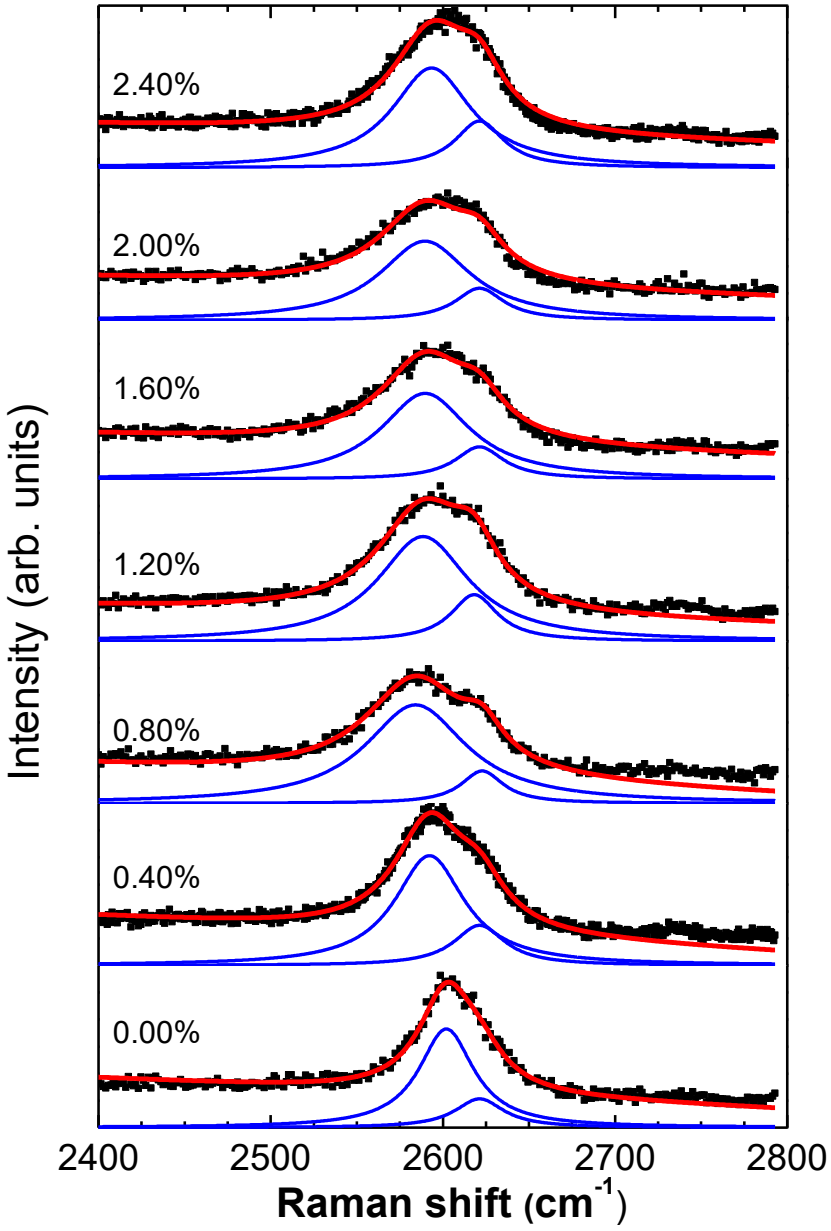

Figure S2: 2D Raman spectra of the graphene-based touch screen as a function of the applied strain (correspond to the data of the first run in Figure 2a, 1st run).

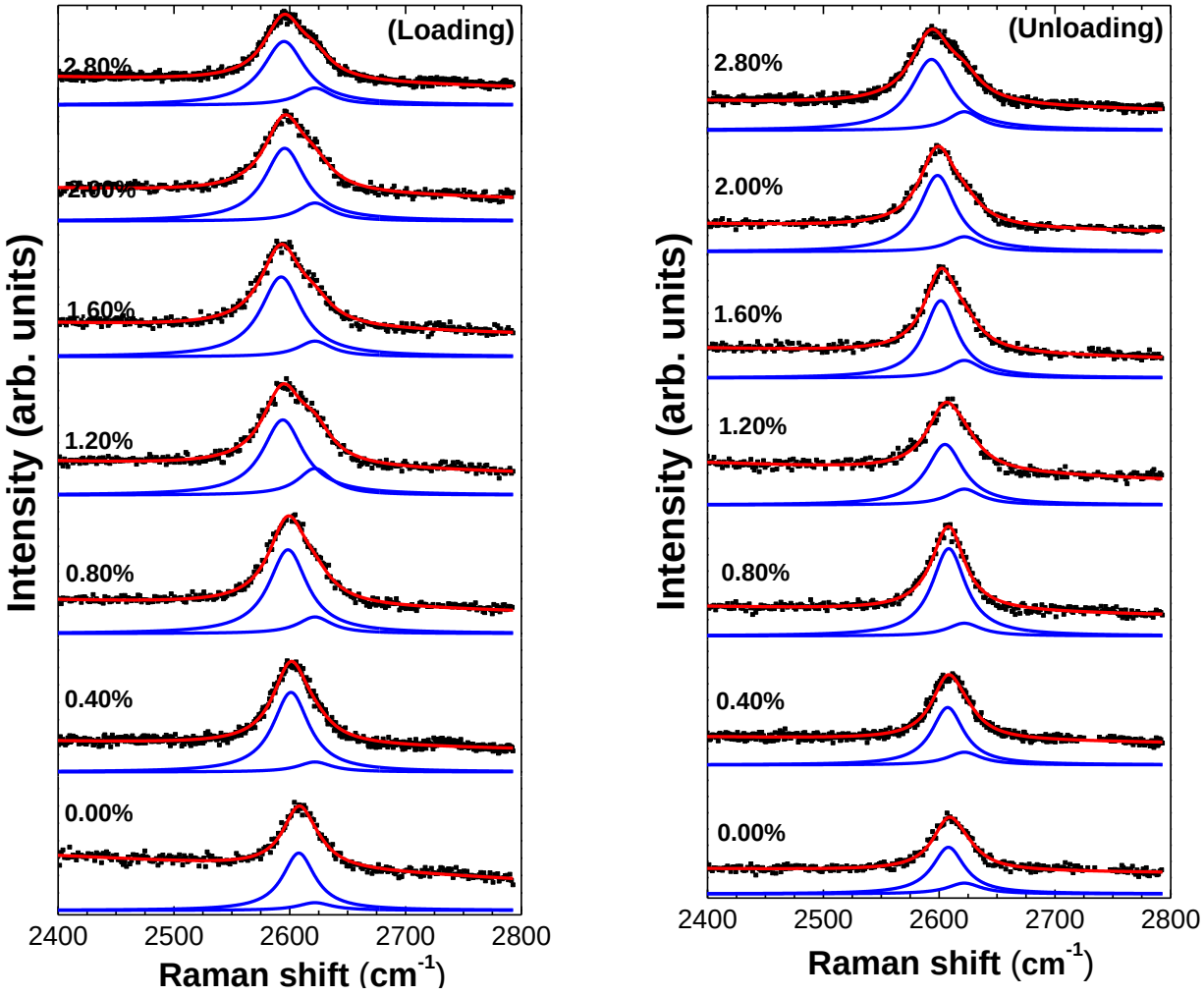

Figure S3: 2D Raman spectra of the graphene-based touch screen as a function of the applied strain (correspond to the data of Figure 2c, 1st cycle).

3. **The dependence of Pos(2D) and the corresponding FWHM(2D) with the applied strain for another sampling area of the flexible display**

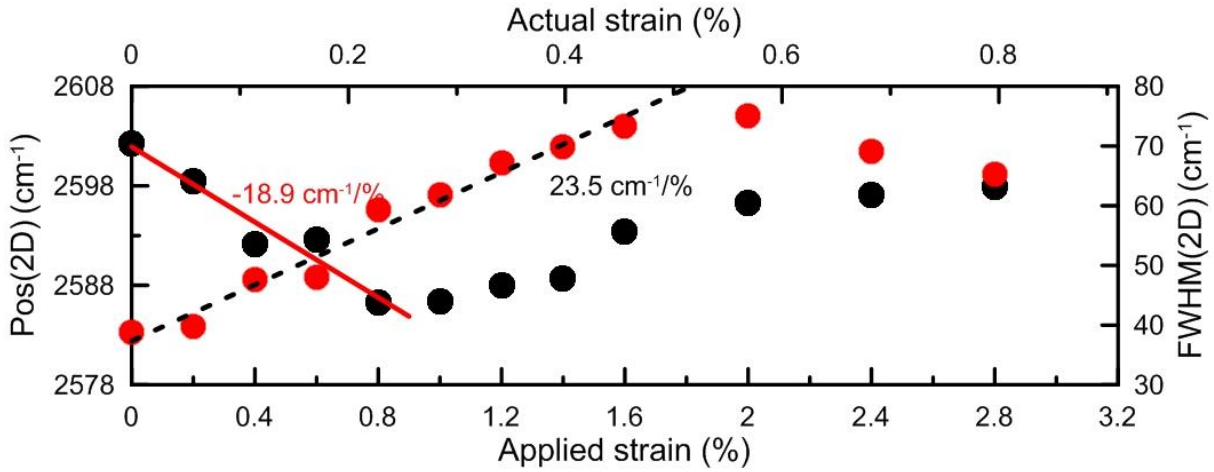

Figure S4: Pos(2D) and the corresponding FWHM(2D) versus applied and actual strain for another sampling area of the flexible display.

4. Description of wrinkled graphene network

As stated in a previous work[1], in which a monolayer CVD graphene sheet was simply-supported on a PET film, scanning electron microscope (SEM) and atomic force microscopy (AFM) images revealed a network of CVD graphene islands separated by wrinkles with a height of around 15 nm. A similar situation is actually shown on the AFM 3D-image (Fig. S5) of analogous specimen of two CVD grown graphene films transferred sequentially one on top of the other are simply-supported on PET film (Fig S5).

As shown therein, wrinkles/folds stick up out of plane and spread all over the examined area. Moreover, isolating the graphene "islands" seem to adhere on the PET substrate, since the corresponding height profile values are low. One should distinguish between grain boundaries and wrinkles. The grain boundaries are defects that lie within the graphene and will not affect the deformation mechanics, whereas the wrinkles are creases or folds that stick up out of plane.

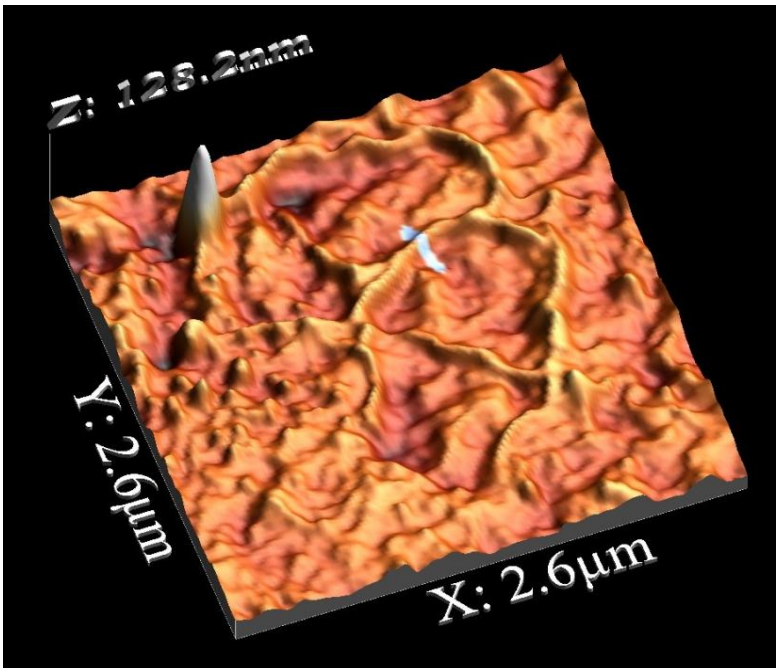

Figure S5: A 3D-AFM image of two CVD grown graphene films transferred sequentially one on top of the other simply-supported on PET film. The corresponding wrinkling network along with the isolated graphene "islands" is clearly depicted.

5. Stress-strain curves for PET and display film

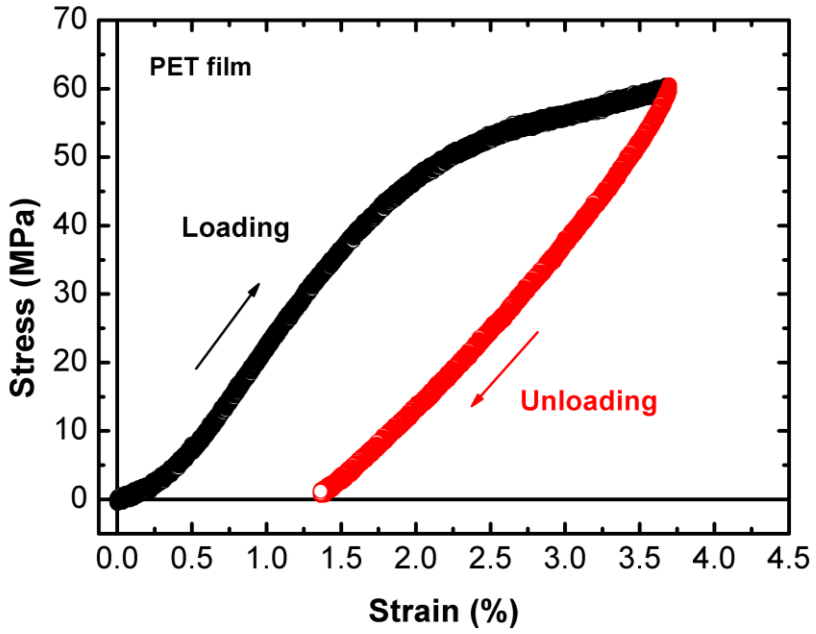

(a)

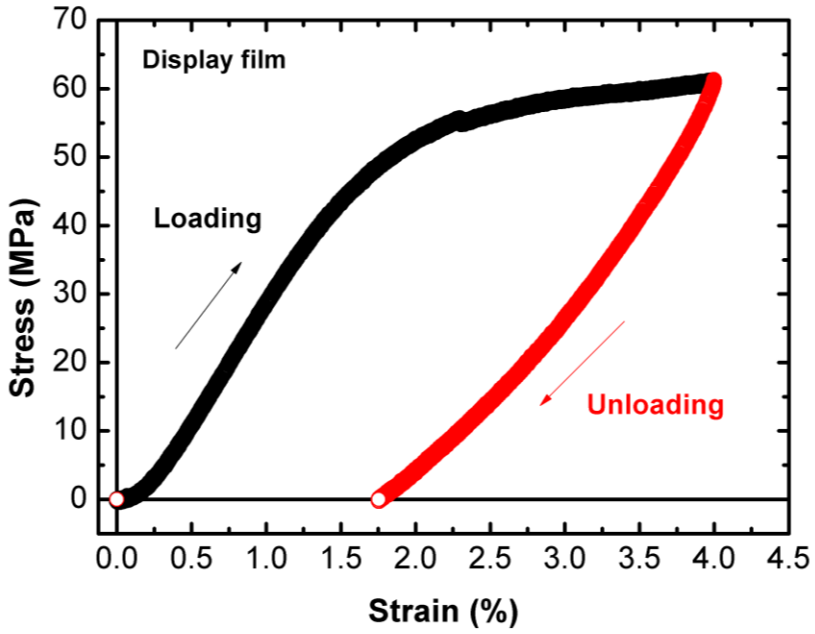

(b)

Figure S6. Stress-strain curves of (a) pure PET and (b) display prototype films.

6. Thermomechanical response of prototype display

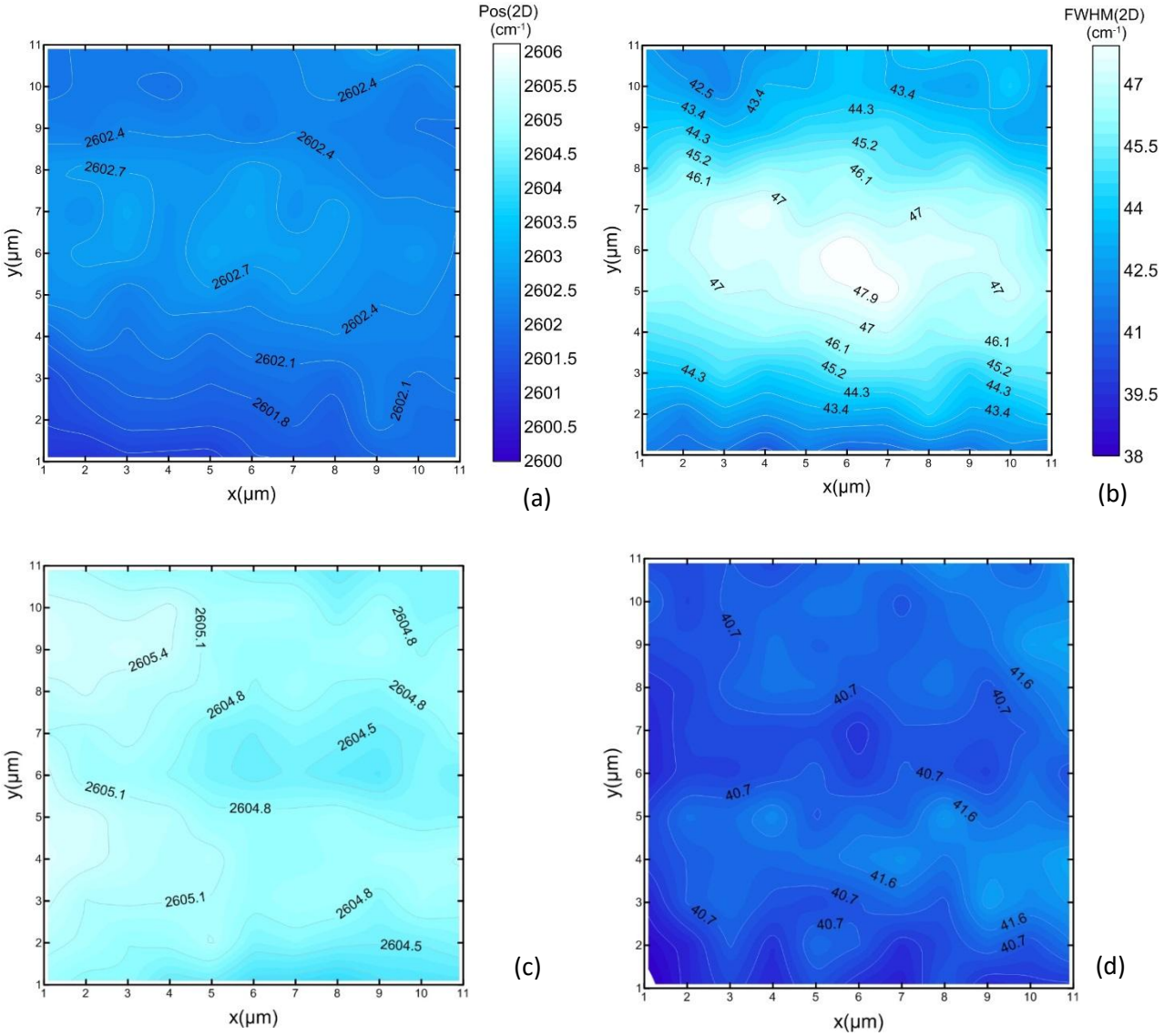

Figure S7. Contour maps of Pos(2D) and FWHM(2D) before (a), (c) and after (b), (d) thermo-mechanical loading at 100 Hz, respectively.

7. Experimental set-up of the functional fatigue test

Figure S8. Experimental set-up to simulate the finger force of a typical user via a mobile stylus over a specimen area of $20 \times 20\ \mu m^2$.

Attention must be paid to the evolution of the maximum compressive (negative) values of each loading cycle (Fig. S9), since they correspond to the actual nature of the experiment which aims to simulate the effect of the 'finger touch' action on the flexible display. The observed shift of the whole range towards positive values must be attributed to the gradual deterioration of the stylus tip polymeric material.

As it was clearly observed during the experiment, after a subsequent number of cycles, the stylus tip adhered to the specimen surface, resulting for the load cell to sense positive values during the upward movement of the hydraulic probe. This behavior must not be correlated to the compressive action of the tip during the downward movement, which constitutes the essence of the experiment. The user finger force simulation is presented on the corresponding video

Video S1: A typical user force simulation via mobile stylus

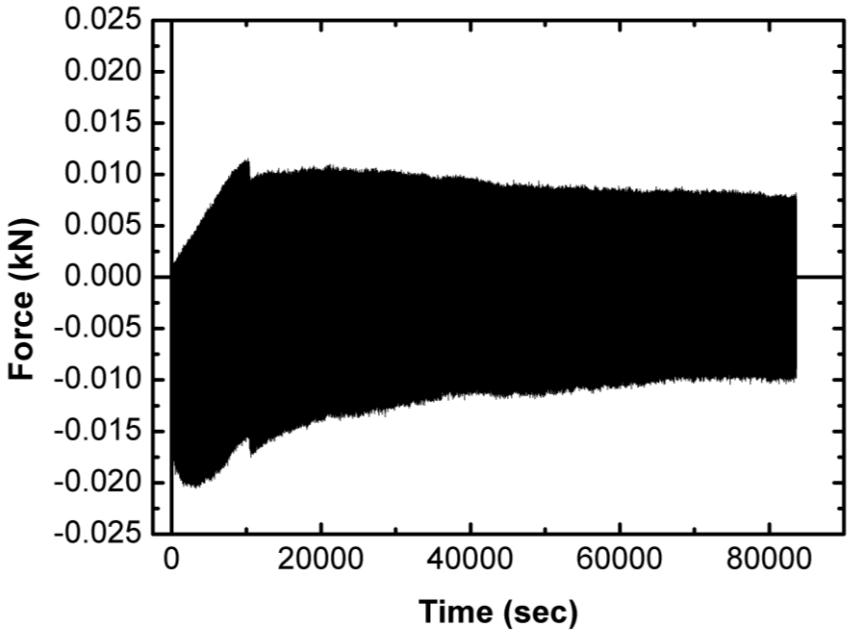

Figure S9. The resulting force on the contact area as a function of the overall duration of the functional fatigue experiment. Simulation of the effect of the 'finger touch' action on the flexible display for initial max applied load of -20N

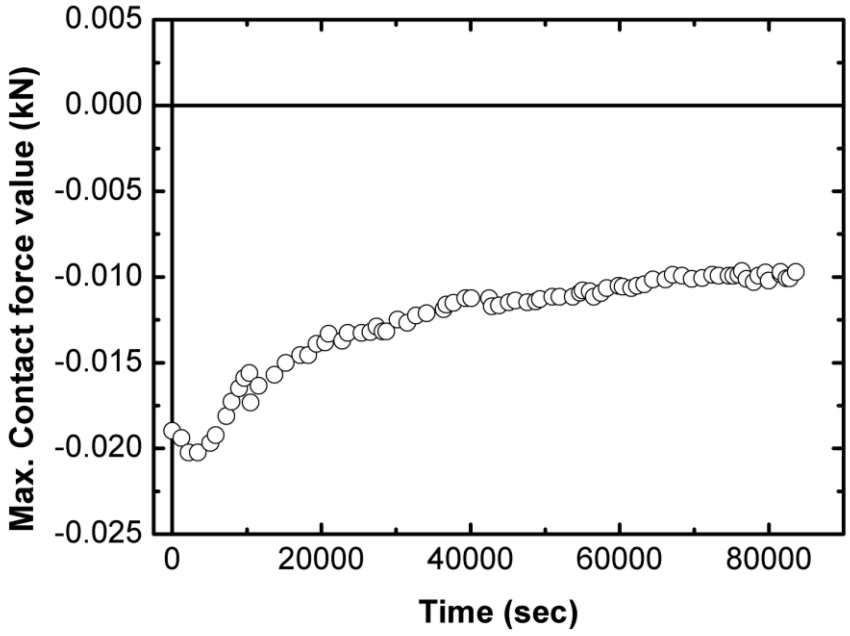

Figure S10. The evolution of maximum contact force as a function of the overall duration of the functional fatigue experiment.

8. Differential Scanning Calorimetry

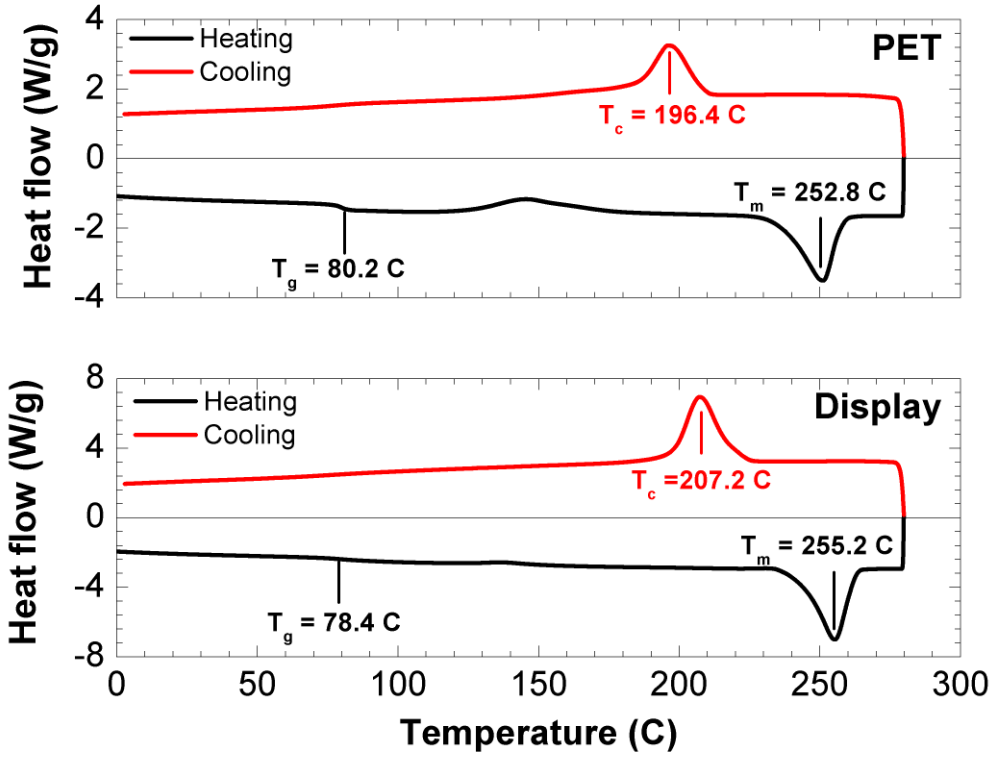

Figure S11. Differential scanning calorimetry thermogram for pure PET film (top panel) and the display prototype (bottom panel) after the second heating run, where the inherent properties of the materials can be evaluated. The corresponding transitions temperatures (T_g: glass transition, T_m: melting, T_c: crystallization) are also depicted.

According to the above thermographs pure PET film shows: (a) a weak glass transition at 80.2 ^{o}C, where a small increase in heat capacity is observed, (b) a cold crystallization at 196.4 ^{o}C (ΔH_c = 25.3 J/g), where the polymer undergoes some small amount of crystallization upon heating and (c) a very clear melting at 252.8 ^{o}C (ΔH_m = 34.5 J/g), where the existing crystalline component is destroyed. Similarly, the display prototype sample shows (a) a very weak glass transition at 78.4 ^{o}C, (b) a cold crystallization at 207.2 ^{o}C (ΔH_c = 38.9 J/g) with a rather broader peak compared to pure PET film and (c) a melting at 255.2 ^{o}C (ΔH_m = 34.6 J/g). Any difference between the pure PET film and the display prototype is attributed to the

complex structure of the later which is actually a “sandwiched” structure where the two layers of CVD graphene are entrapped within two PET films and a thin vinyl acetate (EVA) adhesive layer.

9. Optimal design

In order not to exceed the ultimate strain of graphene (or other 2D materials), we must have:

$$\varepsilon_S + \varepsilon_B < \varepsilon_U + \varepsilon_0 \qquad \text{(S.1)}$$

where the graphene strains due to stretching, bending, ultimate and pre-compressive are appearing respectively.

We can optimize only ε_B and ε_0 since ε_S is the applied stretching and ε_U is a material property. As can be evinced from Fig. 3, the rippling is beneficial since it generates a positive value of ε_0, roughly (1D model) $\varepsilon_0 \approx 2A/\lambda$, where A is the height of the ripples and λ is the distance between two adjacent ripples. In our case of CVD graphene we estimate $\varepsilon_0 \approx 2\%$

Furthermore, considering the display as composed by N+1 layers, each of them with Young's modulus E_i and thickness h_i we can design the system in order to have $\varepsilon_B \approx 0$ in the graphene layer "0" even under pronounced bending. Applying the plate multilayered theory[2] we find that the related optimal position of the graphene layer must be:

$$y_0 = \frac{\sum_{i=1}^{N} E_i h_i y_i}{\sum_{i=1}^{n} E_i h_i} \qquad \text{(S.2)}$$

where y_i are the positions of the centroids of the layers with respect to an arbitrary reference system.

In our case this has been satisfied in the simplest way, i.e. with two symmetric layers, of PET embedding the rippled two layers graphene. These simple mechanical considerations are thus fundamental for designing stretchable and flexible electronics as the case study reported in this paper.

REFERENCES

1. Li, Z.; Kinloch, I. A.; Young, R. J.; Novoselov, K. S.; Anagnostopoulos, G.; Parthenios, J.; Galiotis, C.; Papagelis, K.; Lu, C.-Y.; Britnell, L., Deformation of Wrinkled Graphene. *Acs Nano* **2015,** *9* (4), 3917-3925.

2. Carpinteri, A.; Pugno, N. *Extension of the de Saint Venant and Kirchhoff theories to functionally graded materials*; IOS Press: pp 53-62.